On the Validity of the Quasi-linear Approximation for Turbulent Plasmas

D. Biskamp, H. Welter

IPP 6/94

March 1971

MAX-PLANCK-INSTITUT FÜR PLASMAPHYSIK

GARCHING BEI MÜNCHEN

Abstract

Theoretical conditions for applicability of the quasi-linear theory (QLT) are formulated. To investigate the importance of these conditions, numerical experiments are performed on two different types of weak 1-dimensional plasma instabilities. It is found that the behaviour of the bump-in-tail instability is consistent with QLT (saturation field energy $\langle \tilde{E}^2 \rangle / 8\pi nT \sim$ linear growth rate γ) if these conditions are satisfied, while in the opposite case trapping stabilisation is important (trapped particle bounce frequency $\omega_b \sim \gamma$) The weak symmetric two-stream instability never satisfies the criterion for validity of QLT, since all particles that are supposed to diffuse are trapped ($\Delta v_{diff} \sim \Delta v_{trap}$). Incidentally, however, the first saturation level predicted by QLT is the same as given by the condition for trapping stabilisation $\omega_b \sim \gamma$. The important deviation in this case from weakly turbulent behaviour is apparent from the coherent mode coupling process, which becomes (relatively) the stronger, the weaker the instability.

On the Validity of the Quasi-linear Approximation for Turbulent Plasmas

by D. Biskamp and H. Welter

1) Introduction

The quasilinear approximation is the simplest approach to describe the evolution of certain weak plasma instabilities. It was conceived almost 10 years ago [1, 2] and since then has divided plasma theoreticians into two schools: the practicians who use this approach because of its simplicity (in many cases it is the only practical way) and the sceptics who feel that it is too simple to be reliable, and who have indeed good arguments that the quasilinear approximation is rather doubtful in most cases of practical interest. With the advance of computer simulation of collision-free plasma dynamics the computational plasma physicists have joined the discussion as a third group. Looking at their numerical results, they normally see a behaviour quite different from the prediction of quasilinear theory and thus claim to have "proved" that this approach is not correct and should be revised. However, in many numerical experiments the conditions are clearly outside the applicability range of this approximation and hence the observed discrepancy is not so surprising. Clarification of this somewhat confused situation seems to be useful. In this note we shall first summarize the theoretical conditions for validity of the quasilinear approach. To see how critically the behaviour

of the instability depends on these conditions we then study two well-known types of instabilities, the bump-in-tail configuration and the weak symmetric two-stream instability, by a set of numerical simulation experiments.

The basic equations to describe a turbulent collision-free plasma are the equations for the mean distribution functions $f_{0j} = \langle f_j \rangle$,

$$\frac{df_{0j}}{dt} = -\frac{e_j}{m_j} \frac{\partial}{\partial \underline{v}} \langle \tilde{\underline{E}} \tilde{f}_j \rangle \quad , \tag{1}$$

and the fluctuating part of f_j , $\tilde{f}_j = f_j - f_{0j}$

$$\frac{d\tilde{f}_j}{dt} + \frac{e_j}{m_j} \tilde{\underline{E}} \frac{\partial f_{0j}}{\partial \underline{v}} = -\frac{e_j}{m_j} \frac{\partial}{\partial \underline{v}} \cdot \left[\tilde{\underline{E}} \tilde{f}_j - \langle \tilde{\underline{E}} \tilde{f}_j \rangle \right] . \tag{2}$$

Here d/dt is the zero order Vlasov operator for the time change along the unperturbed particle orbits taking into account inhomogeneities and external fields. The first assumption in the quasilinear approximation is to neglect the nonlinear term in Eq.(2). The next step consists in introducing a scaling into the truncated Eq.(2), considering spatial and temporal changes of f_{0j} and the external fields negligible over typical wavelengths and periods of the fluctuating quantities $\tilde{f}_j$, such that in solving Eq.(2) f_{0j} is considered a known function of $\underline{v}$. This scaling is the origin of the irreversible (diffusion-like) behaviour which the usual quasi-

linear equation describes as compared to the reversible system (1) and (2) (even in the truncated form). The solution of the linear part of (2) contains the usual e^{ikvt} – contributions originating from the initial perturbations. These are assumed to be negligible in the equation for f_{0j} as compared to the $e^{-i\omega_k t}$-terms, which is only possible for growing modes. The resulting system can be written in the form:

$$\frac{df_{0j}}{dt} = \frac{\partial}{\partial \underline{v}} \cdot \underline{\underline{D}}_j \frac{\partial f_{0j}}{\partial \underline{v}} \quad , \quad \underline{\underline{D}} \{ |E_{\underline{k}}|^2, \underline{v} \} \tag{3}$$

$$\dot{|E_{\underline{k}}|^2} = 2\gamma_{\underline{k}} |E_{\underline{k}}|^2$$

The system (3) is in general useful only in 1-dimensional cases. For multi-dimensional problems the equations are not only hard to tackle, there is also some doubt about their significance in these cases. Since as a rule there is no stationary solution of (3) with $|E_k|^2 \neq 0$ in 2- or 3-d [3], it can be indirectly concluded that eventually the modes must be damped, in which case the problem of the e^{ikvt}-parts of $\tilde{f}_j$ will arise. We shall therefore consider only 1-dimensional problems here. The general time evolution predicted by the system (3) is well known:

1) f_{0j} is changing in a diffusive way, flattening peaks, filling wells, with a tendency to form a plateau.

2) The mode energies $|E_k|^2$, initially

increasing exponentially are stabilized, remaining constant. The same is of course true of the total fluctuation energy $\langle \tilde{E}^2 \rangle / 8\pi$.

2) Theoretical conditions for quasi-linear behaviour

In this section we state some conditions that should be satisfied to justify a quasi-linear approach and describe briefly what is believed to occur if these conditions are violated.
Since in the quasilinear approximation the main part of the nonlinear interaction, the mode coupling, is neglected, it is evident that the instability has to be sufficiently weak. This can be expressed as a requirement on the growth rate, e.g. $\gamma/\omega_p \ll 1$ for electrostatic instabilities, or more adequately as a condition on the saturation value of the fluctuation energy compared to the thermal energy, $\langle \tilde{E}^2 \rangle_s / 8\pi nT \equiv W_s \ll 1$.
W_s is related to the free energy available to drive the instability, which should be sufficiently small.

The irreversible character of the quasi-linear approximation, which is evident from the diffusion equation (3), requires the presence of some random or stochastic process. In a collisionless system such a process can only be provided by a stochastic nature of the

instability. Hence as a necessary condition there must be a sufficiently broad spectral range Δk of unstable waves.

For a nonresonant instability, if a large part Δv of the distribution function is affected, randomization is introduced by scattering of the particles by a stoachastic wave pattern of correlation length $\sim (\Delta k)^{-1}$. This process is similar to the scattering of electrons by the randomly distributed ions in a Lorentz gas. A condition for the validity of the diffusion approximation is $v_0 \Delta k \gg \gamma$, where v_0 is a typical velocity from the range Δv.

In the case of a resonant instability the particles most affected by the instability are located near the phase velocity of a wave. In order to have these particle moving stochastically, the wave pattern itself must change in a random way. Hence the unstable waves have to be dispersive, with a sufficiently broad range of phase velocities $\Delta \omega/k$, such that $k_0 \Delta \omega/k \gg \gamma$, where k_0 is a typical value of the spectrum Δk. If the diffusion process is not effective, the stabilization is said to be due to particle trapping. The idea of trapping refers to a coherent wave, catching particles while growing and swirling them around in phase space. This ordered motion is perturbed by any

change of the wave pattern and becomes quite random if the correlation time of the wave is smaller than the bounce period $\sim \omega_b^{-1}$ of a trapped particle. Hence a "nonlinear" condition for "diffusive" behaviour of the particles is $k_0 (\Delta \omega/k)_s > \omega_b$, where $\omega_b^2 = \frac{e}{m} k_0^2 \phi_s$, $(\Delta \omega/k)_s$ is the range of phase velocity of the spectrum at the saturation time and ϕ_s is the saturation potential amplitude. This implies a condition on the initial fluctuation level. Since $\gamma(k)$ is a continuous function with a maximum value at k_0 (Fig. 1a), an initially broad spectrum W_0 (Fig. 1b) will become more and more peaked around k_0 (Fig. 1c), the longer the phase of linear growth lasts. Thus a broad $(\Delta \omega/k)_0$ will shrink essentially to a single mode, $(\Delta \omega/k)_s \approx 0$ at saturation time, if W_0/W_s is too small. In this case trapping must be the main stabilization mechanism.

In this case an estimate of the saturation energy can be obtained by arguing that the particles should be turned around by the wave in a linear growth time, $\omega_b \sim \gamma$.

In the case of a nonresonant instability the "nonlinear" condition for trapping effects to be unimportant is that the number of trapped particles be small as compared to the number of diffusing particles,

$$\Delta v_{tr} \ll \Delta v_{diff} \quad , \quad \Delta v_{tr}^2 = 2e\phi_s/m \; .$$

These conditions and implications can be tested in numerical experiments by comparing the experimental behaviour of $f_{0j}(t)$, $\langle \tilde{E}^2(t) \rangle$, $|E_k(t)|^2$ with the theoretical predictions and investigating the dependence of these quantities, in particular the saturation field energy W_s, on the type of instability, the growth rate, and the initial conditions.

3) The bump-in-tail instability

As the prototype of a resonantly unstable system we consider the bump-in-tail configuration. We shall first show that the usual criterion for weakness of an instability mentioned in section 2), $\gamma/\omega_p \ll 1$, which is convenient since it refers to the linear quantity γ, is not very significant, and that it is necessary to know the saturation level W_s in order to estimate the importance of the nonlinear term.

In Table 1 we compare the growth rate γ_{max}/ω_p and saturation energy W_s for two bump-in-tail configurations of the form

$$f_0(v) = \frac{1-n_b}{\sqrt{2\pi}} e^{-v^2/2} + \frac{n_b}{\sqrt{2\pi}\, v_b} e^{-(v-u_b)^2/2v_b^2} \tag{4}$$

with different drift u_b and thermal spread v_b of the beam.

Table 1

n_b	u_b	v_b	γ_{max}	W_s
5 %	6	2	5.3×10^{-3}	1 %
5 %	3.7	0.7	6×10^{-2}	0.18%

Although the growth rates are approximately equal, the values of the saturation energy W_s (here W_s is the electric energy over the <u>total</u> energy) are quite different.[+)] Since even in strong electrostatic instabilities only a few percent of the free energy is transformed into electric energy, the upper case in Table 1, drawing 5, with W_s = 1 %, shows that conclusions from the smallness of the growth rate, $\gamma/\omega_p \ll 1$, about the weakness of the instability is dangerous.

+) This can be understood qualitatively since the free energy, characterized by the kinetic energy of the bump, is much different. Particles must diffuse over a much longer distance in v-space in the upper case to form a plateau in f_0 .

In continuation of the extensive numerical work on the bump-in-tail instability, especially by Dawson and Shanny [4] and Morse and Nielson [5], we performed a number of numerical experiments, using the PIC (particle-in-cell) method as described in detail by Morse and Nielson[5]. We wanted to study the behaviour of the very weak instabilities in a more systematic way, varying the growth rate only by changing the strength of the bump n_b, keeping drift velocity u_b and thermal spread v_b constant, so that the type of instability is changed as little as possible. We consider an initially homogeneous system with an electron velocity distribution as given in Eq.(4), with $u_b = 3.68$, $v_b = 0.7$ and $n_b = 4\,\%,\ 5\,\%,\ 7{,}5\,\%,\ 10\,\%$. All four cases are sufficiently weakly unstable, with unstable modes having a broad range of phase velocity $\Delta\omega/k$, $k_0 \Delta\omega/k > \gamma$, as can be seen from Table 2. To be definite we take k_0 such that $\gamma(k_0) = \gamma_{max}$ and $\Delta\frac{\omega}{k} = \frac{\omega(k_1)}{k_1} - \frac{\omega(k_2)}{k_2}$, k_1, k_2 such that $\gamma(k_1) = \gamma(k_2) = \frac{1}{2}\gamma_{max}$ as indicated in Fig.1

Table 2 [+)]

n_b	γ_{max}	k_0	$k_0 \Delta\frac{\omega}{k}$
4 %	0.047	0.30	0.175
5 %	0.06	0.30	0.185
7,5 %	0,087	0,29	0.2
10 %	0,107	0.29	0.196

+) γ, $k_0 \Delta\omega/k$ in units of ω_p, k in λ_D^{-1}

We should emphasize that it is not sufficient to make the second beam weak without considering its thermal spread and drift velocity. Most cases treated previously by particle simulation with typical $n_b = 5\ \%$ can be seen to be outside the validity range of the quasi-linear approximation, γ being quite substantial ($> 0.1\ \%$), the saturation energy rather high ($> 1\ \%$), and $k \Delta \omega/k < \gamma$. When simulating an infinite plasma the computed system should be long enough, so that the discreteness of the k-spectrum is negligible. In the present cases we choose $L = 1000\ \lambda_D$, so that there are typically 50 linearly unstable modes. Much smaller system lengths are found to be inadequate; with $L = 100 - 200\ \lambda_D$, as often used in previous simulation work [3, 4], the discreteness of the k-spectrum is rather strongly pronounced, so that normally a single mode will dominate in the nonlinear phase. The number of particles per Debye cell, $n \lambda_D$, used in these experiments ranges from 200 to 800. The point of using such large numbers is not to reduce the collision frequency, which is small in 1-dimensional plasmas, $\nu_c \sim (n \lambda_D)^{-2}$, but to keep the thermal fluctuation level low enough, $W_0 / W_s \ll 1$, so that the collective oscillations can clearly be distinguished from the thermal noise. To prove or disprove the validity of the quasilinear approximation, we want to investigate the behaviour of the total electrostatic field energy $\langle \tilde{E}^2 \rangle / 8\pi nT \equiv W$, the energy of the single modes

$|E_k|^2/8\pi nT = W_k$ and the average distribution function f_o, varying the strength of the instability, i.e. γ, and the initial perturbation level W_o, i.e. the level of thermal noise. We first carry out a set of numerical experiments where we choose W_o only a few e-foldings below the saturation level, $\ln W_s/W_o < 4$. The behaviour of $W(t)$ for the different beam densities is shown in Fig. 2 a-d. While cases a) and b) are qualitatively consistent with a quasilinear behaviour, there is an increasing discrepancy towards higher beam densities, case c) and especially case d), which show (though not very strongly) an "overshoot" of W at saturation. This "overshoot", which has been reported in most of the previous simulation work on the bump-in-tail instability, is just the first half-cycle of a trapped particle oscillation, and its appearance indicates that coherent trapping plays an important part in the stabilization process. Thus one may interpret the overall behaviour of W in Fig. 2 such that for the weakest case a) trapping effects are small but become increasingly important towards stronger instabilities.

To investigate the condition $k_o(\Delta\omega/k)_s > \omega_b$, mentioned in section II, we determined $k_o(\Delta\omega/k)_s$ from the correlation time near saturation by measuring the correlation function $g(t_o,\tau) = \int dx\, \tilde{E}(x,t_o)\tilde{E}(x,t_o+\tau) / \int dx\, \tilde{E}^2(x,t_o)$. In Fig. 3 $g(t_o,\tau)$ is shown for $n_b = 5\,\%$. The decay time is roughly $10\,\omega_p^{-1}$, hence $k_o(\Delta\omega/k)_s \approx .1\,\omega_p$.

On the other hand we find from the saturation fluctuation energy $W_s = 1.75 \cdot 10^{-3}$ (see Table 3) that $\omega_b \approx .1$. Hence both are approximately equal, and the weak turbulence assumption that trapping is negligible is only marginally valid. Because of the very weak dependence of ω_b on W_s, $\omega_b \sim W^{1/4}$, it is clear that the turbulent energy must be extremely small to make ω_b clearly smaller than $k_0 (\Delta \omega/k)_s$, so that in practically all cases of interest the condition is not satisfied in the strict sense. Since, on the other hand, the behaviour of W_s for $n_b \leq$ 5 %, Fig.2, a, b , is consistent with the quasilinear approximation, it seems that the criterion mentioned above is too strict and should be relaxed to $k_0 (\Delta \frac{\omega}{k})_s \gtrsim \omega_b$ For cases Fig.2, c, d $k (\Delta \omega/k)_s$ is somewhat smaller than ω_b , and hence trapping certainly plays a stronger role.

To investigate the influence of trapping from a different point of view, we measure the dependence of the saturation energy W_s on the growth rate γ, $W_s \sim \gamma^\alpha$. From the quasi-linear equation one would expect $W_s \sim \gamma$, i.e. $\alpha \approx 1$, while in the case of trapping stabilization the particles should be turned around in phase space during one linear growth time, $\omega_b \sim \gamma$, where ω_b is the bounce frequency, which would give a relation $W_s \sim \gamma^4$. Of course, the numerical factors are unknown, and hence a single experiment or several uncorrelated experiments are of no

use. Since, however, we varied the growth rate without changing the type of instability, we can hope that on comparing the results of two experiments a, b the numerical factors will essentially drop out and the ratio $W_s^a / W_s^b = (\gamma^a/\gamma^b)^\alpha$ can provide a relevant value of α. The results are given in Table 3. Since in the presence of a broad spectrum the linear growth rate is different from γ_{max}, we have used in Table 3 the effective growth rate determined experimentally from the curve W(t). We find that α is rather close to one for the weakest instability considered, increasing significantly with increasing γ and W_s, which would be consistent with the interpretation of Fig.2 a-d, mentioned above, that for the strongly unstable cases c) and d) trapping becomes more important. To make the argument convincing it would have to be shown that in the case of strong trapping the relation $W_s \sim \gamma^\alpha$ is valid with α close to 4. Since, however, the relation $\omega_b \sim \gamma$ is not a strict, but at most a qualitatively valid condition, and since the relation $W_s \sim \gamma^4$ is derived from $\omega_b \sim \gamma$ by taking the fourth power, thus strongly enhancing slight changes of the numerical factor which will no longer cancel when comparing different experiments, we shall be content to find α closer to 4 than to 1 for strong trapping. As explained in section 2, trapping can always be made more important merely by reducing the initial perturbation level. As an example Fig.4 shows the behaviour of W for case c), $\eta_b = 7.5\ \%$.

Table 3

η_b	γ	W_s	W_s^a/W_s^b	γ^a/γ^b	α
4 %	0.022	0.10 %	1.7	1.47	1.4
5 %	0.033	0.17 %			
7.5 %	0.049	0.36 %	2.1	1.48	1.85
10 %	0.059	0.65 %	1.8	1.2	3.1

with the thermal level reduced by a factor of 10 as compared to the case shown in Fig.2c. In contrast to Fig.2c the overshoot is clearly pronounced here. To force the system to show extreme single mode behaviour and consequently a pure trapping case, we shortened the system length, so that only one mode, the one with the maximum growth rate, was linearily unstable. In Table 4 the results of a set of simulation calculations are given for the same distribution functions as used in the different cases of Table 3, but with initial conditions corresponding to single mode growth. Here γ is the maximum growth rate γ_{max} of Table 2, and W_s in the second column is an average value over several similar runs that differ only in the initialization.

Table 4

n_b	γ	W_s	W_s^a/W_s^b	γ^a/γ^b	α
4 %	0.047	0.110 %	1.68	1.28	2.1
5 %	0.06	0.185 %	2.5	1.45	2.46
7.5 %	0.087	0.465 %			
10 %	0.11	0.86 %	1.85	1.26	2.66

In these single mode cases α is definitely larger than 1. For the weaker instabilities considered, a) b), the exponent α is clearly different in this case from that of a broad spectrum, Table 3, while for the more strongly unstable cases, c), d), the difference becomes small. The exact numbers given in Tables 3, 4 should of course not be taken too seriously. W_s varies when starting with different statistical initializations, but the variation is scarcely larger than 5 %.

According to weak turbulence theory, the slow decay of the wave spectrum, seen in Fig.3, should be due to nonlinear wave-particle scattering since resonant 3-wave mode coupling is forbidden. The decay of Langmuir turbulence has been treated in detail, see Kadomtsev IV.1.[6]. However, because of the particular shape of the distribution function (see Fig.7) these results are not applicable in our case. The waves cannot diffuse in k-space to $k = 0$ since the part in v-space where f_0 drops from the plateau to zero,

$f_0' < 0$, constitutes a region of significant Landau absorption. Hence we suggest the following process of wave decay without carrying out the tedious work of solving the kinetic wave equation. Waves diffuse in k -space toward smaller k-values, which means larger phase velocities, until they reach the end of the plateau, where absorption sets in. In contrast to the decay of Langmuir waves in a single humped Maxwellian distribution, the wave energy will not remain constant, but decay. Analyzing the wave spectrum, the process of mode diffusion in k -space can clearly be seen for the more strongly unstable cases in Fig. 2c, d, while it is nearly imperceptible in the weakly unstable cases a, b. If this turbulent mode scattering is the main source of decay of the wave spectrum, the decay rate should be of the order of W and should be approximately proportional to W. It can be measured from Fig. 2 that this is roughly true.

In contrast to the total fluctuation energy W , the single modes W_k do not, in general, show a smooth, "quasi-linear" behaviour. They rise or decay rather abruptly, which cannot be explained by turbulent mode coupling or nonlinear wave-particle scattering. Their time variation does not decrease towards larger system sizes, i.e. by increasing the number of modes and decreasing their distance $dk = 2\pi/L$. However, the

fluctuations of W_k are not completely random. By analyzing the wave spectrum more closely, it is frequently found that, if a certain mode is decaying, some mode close to it rises so that their sum is approximately constant. One explanation would seem to be that it is not single Fourier modes but rather wave packets with a certain width $\Delta k \gg dk$ that are the real physical elements of the turbulence, where Δk is some function of W which should decrease with decreasing W. Modes within Δk are no longer independent. A small spatial distortion of a wave train shifting the mean wave length by a small fraction gives rise to a sudden decay of a mode, while some neighbouring mode is growing. Summing neighbouring modes in an appropriate way leads to "supermodes", which behave much more smoothly with time than the individual Fourier modes.

In the development of the instability, especially for the more strongly unstable cases, these supermodes tend to sharpen, i.e. the spectrum, initially quite smooth, has a tendency to develop a small number of peaks, where the central mode of a supermode grows at the expense of its neighbor modes. This phenomenon can be interpreted as mode locking, a mode growing rapidly at the expense of its neighbors. If the spectrum is rather narrow, often only a single mode is growing strongly (there is only a single supermode then), leading to the overshooting trapping oscillation usually seen in previous simulation work. In Fig. 6 an example is shown

of a broad spectrum disintegrating into several super-modes.

In contrast to the fluctuation energy the behaviour of the average distribution function does not depend sensitively on the form of the spectrum. This behaviour has already been found in previous simulation calculations [4], and it is not very surprising since velocity space diffusion and coherent trapping have essentially the same effect on f_0, filling up the well between the bump and the bulk of the distribution. In all four cases considered $n_b = 4\ \% - 10\ \%$, the plateau formation was nearly perfect. Since the instabilities are weak, the distribution is noticeably changed only in the plateau, where the unstable phase velocities are located. Outside this resonance region the change of the distribution function $\Delta f_0 = f_0(\infty) - f_0(0)$ goes to zero very rapidly, Δf_{02} and Δf_{03}, defined in Fig.8, being hardly perceptible in the real plots of the distribution function (see Fig.7). They can be ascribed to nonresonant diffusion (see Ref.6). In the usual version of the quasilinear treatment of the bump-in-tail instability, the energy integral predicts that half of the kinetic energy lost by the small bump owing to the plateau formation is transformed into electric energy, and half into heating of the main bulk. We can revise this picture somewhat. As mentioned above, the distribution function is deformed only in the immediate neighbourhood of the plateau. Since the particle numbers

$n_2 = \int dv\, \Delta f_{02}$ and $n_3 = \int dv\, \Delta f_{03}$ are about equal, it is evident that the main contribution to the energy redistribution comes from Δf_{03} because of the higher velocity. We measured $E(v) = \int_{-\infty}^{v} dv\, \frac{v^2}{2} \Delta f_0$, which is qualitatively plotted in Fig.8. The main part of the energy obtained by plateau formation, $E_{max} - E(\infty)$, goes into heating the bump, while the temperature increase of the main bulk is negligible. The fraction $E(\infty)/E_{max}$, $E(\infty)$ being equal to the electric energy by energy conservation is smaller than 1/2 ($\sim$ 20 %) because of the different dispersion relation (the usual factor 1/2 comes from the dispersion relation $\varepsilon(\omega) \approx 1 - \frac{\omega_p^2}{\omega^2}$, where because of $\omega \frac{\partial \varepsilon}{\partial \omega} = 2$ the kinetic part of the turbulent energy is equal to the electric part). Another interesting feature we noticed is the change of Δf_0 and of $E(v)$ in the decay phase of the spectrum after saturation. Most of the energy lost by the electric oscillations goes into the change of Δf_{03}, which is consistent with the picture, described above, that the waves are absorbed at the upper edge of the bump, where $f_0' < 0$.

4) The symmetric two-stream instability

A characteristic feature of many nonresonant instabilities is that there is little or no dispersion, $\Delta \frac{\omega}{k} \ll v_{th}$ or, more precisely, $k \Delta \frac{\omega}{k} \lesssim \gamma$. Since here the wave

pattern does not change stochastically, those particles which provide for the main contribution to the stabilizing diffusion process, must cover a sufficiently large region Δv in velocity space. The classical example is the firehose instability, where the idea of nonresonant quasilinear diffusion was first introduced by Shapiro and Shevschenko[7]. Here the resonant denominators $(kv-\omega)^{-1}$ cancel and the diffusion coefficient contains only positive powers of v. Unfortunately however this seems to be an exception. In a number of instabilities the δ-function contribution is absent because of symmetry properties of the distribution function, but the diffusion coefficient strongly depends on v in the vicinity of the wave velocity. As an example we consider the symmetric two-stream instability of two equal warm electron beams near the marginal drift velocity, see Fig.9. The phase velocity of the unstable waves is exactly zero. Hence the quasilinear equation (3) becomes approximately

$$(5)\qquad \frac{\partial f_0}{\partial t} = \frac{e^2}{m^2}\frac{\partial}{\partial v}\sum_k \frac{|E_k|^2}{i(kv-i\gamma_k)}\frac{\partial f_0}{\partial v} \approx \frac{e^2}{m^2}\frac{\partial}{\partial v}\sum_k \frac{\gamma_k |E_k|^2}{k^2}\frac{1}{v^2}\frac{\partial f_0}{\partial v}$$

which can be written in the compact form:

$$(6)\qquad \frac{\partial f_0}{\partial h} = \frac{\partial}{\partial v}\frac{1}{v^2}\frac{\partial f_0}{\partial v}, \quad \text{with} \quad h = \frac{1}{2}\frac{e^2}{m^2}\sum_k \frac{|E_k|^2}{k^2}.$$

Equation (6) can be solved exactly yielding $f_0(v,h)$ in terms of the initial distribution; however, the analytical expression is rather complicated and shall not be given

here. Instead we discuss Eq.(6) qualitatively. The main diffusion effect occurs near the origin, making the distribution flat, as shown in Fig.9; the diffusion stops when $f_0(v,h)$ has become marginally stable.

Let us investigate this behaviour more closely for the case where the distribution function consists of two equal Maxwellians:

$$(7) \qquad f_0(v,0) = \frac{1}{2}\frac{1}{\sqrt{2\pi}}\left(e^{-\frac{(v+u)^2}{2}} + e^{-\frac{(v-u)^2}{2}}\right)$$

(v, u normalized to the thermal velocity).
The critical value of the drift velocity u is $u_c \approx 1.3$, and we shall consider slightly unstable systems, $u - u_c = \varepsilon \ll 1$. The instability is switched off if, according to the Penrose criterion,

$$(8) \qquad \int \frac{f_0(v,h) - f_0(0,h)}{v^2}\, dv = 0$$

Using the distribution function shown in Fig.9b, Eq.(8) yields $v_1 \approx \sqrt{2\pi}\,\frac{2u}{u^2-1}\,e^{u^2/2}\,\varepsilon \sim \varepsilon$. Since from Eq.(6) $h \sim v_1^4$, we find $h \sim \varepsilon^4$. The linear growth rate for the distribution (7) for weakly unstable drift is approximately $\gamma \approx \sqrt{\frac{2}{\pi}}\,\frac{e^{u^2/2}}{u^2-1}\,k\left(\frac{\varepsilon}{u} - k^2\right)$ and the maximum value $\gamma_{max} \equiv \gamma_{k_0} \sim \varepsilon^{3/2}$ with $k_0 \sim \varepsilon^{1/2}$. Hence we find the saturation level:

$$(9) \qquad h \sim \tilde{\phi}_s^2 \sim \varepsilon^4 \,, \quad W_s \sim \tilde{E}_s^2 \sim \gamma^{10/3}$$

Since essentially the particles with $v \leq v_1 \ll v_{th}$ are affected by the diffusion process, a necessary condition for applicability of the quasi-linear approximation is $v_1 \gg \Delta v_{tr}$. However, from the preceding consideration $\Delta v_{tr} \sim \sqrt{\phi} \sim v_1$. Hence all particles that should diffuse by being scattered by a random wave pattern are indeed trapped within a single potential well. This behaviour is independent of the growth rate, which means that also for very weakly unstable systems stabilization should occur by trapping of particles, i.e. coherent rather than turbulent behaviour should dominate. Mathematically this can be seen from Eq.(2) where for $v \leq v_1$ no different time scales can be distinguished, $k v_1 \sim \gamma$. Hence the conclusions drawn from quasi-linear theory, especially the result Eq.(9), are not reliable.

Surprisingly the amplitude for trapping stabilization given by the condition $\omega_b \sim \gamma$, as mentioned in section 2, leads to the same $W_s(\gamma)$ relation as obtained from the quasilinear equation, namely $W_s \sim \gamma^{10/3}$, Eq.(9). In this respect quasilinear and trapping behaviour are indistinguishable.

To study the nonlinear evolution of this instability we have carried out a set of numerical experiments using the distribution (7) as initial condition for three different cases. The parameters are found in Table 5.

Table 5

u	γ_{max}	k_0
1.45	0.032	0.17
1.5	0.045	0.188
1.55	0.059	0.204

System length was $L = 300\ \lambda_D$, and the number of simulation particles ranged from 2×10^5 to 8×10^5. The results for the fluctuation energy W and the potential $V = \frac{\langle \tilde{\phi}^2 \rangle}{8\pi}$ are shown in Figs 10 and 11. While for the more strongly unstable case $u - 1.55$ $W(t)$ to some extent shows the familiar features with linear growth, saturation and slower decay, the weaker instabilities exhibit an increasingly different behaviour. There is a first saturation level, after which W tends to rise further. This is more clearly seen by considering the behaviour of V, Fig. 11. Since this quantity enters the quasi-linear equation, it is evident that there is no real quasi-linear behaviour. From a spectral analysis it is seen that the further increase of V is due to the decay of the strongest mode and simultaneous increase of the mode with about half the wave number, which is the same phenomenon as the coalescence of phase space vortices, described by Morse and Nielson [5] in the case of the strong two stream instability (in our case phase space plots do not show any significant structure because of the much weaker instabilities considered). This is a strong, coherent (not turbulent) mode coupling effect, which becomes relatively the more pronounced the weaker the instability, as seen from Fig 10 . Comparing the first saturation level which W reaches at $t = t_0$ for the three cases considered, the result is consistent with Eq.(9). However, the distinction between a quasi-linear and a mode coupling phase becomes rather artificial.

Conclusions

To investigate the conditions for validity of the quasi-linear approximation, we numerically considered two types of weak electrostatic instabilities: the resonant bump-in-tail instability and the nonresonant weak symmetric two-stream instability. In the first case it was seen that for a sufficiently small and gentle bump the main features of Q.L.T are verified in the numerical simulation experiments, if the initial conditions are such that at saturation time the spectrum is sufficiently broad, with $k(\Delta\frac{\omega}{k})_s \gtrsim \omega_b$. With these conditions the electric fluctuation energy $W = \langle\tilde{E}^2\rangle/8\pi nT$ does not, in general, show the pronounced "overshoot" known from previous simulation work, and the following slow decay rate is roughly proportional to W. If unstable system is started from a much lower thermal fluctuation level, the nonlinear spectrum is strongly peaked and the trapping oscillation overshoot is clearly seen. This dependence on the initial perturbations implies severe restrictions if one tries to satisfy the quasi-linear conditions strictly on a real experimental set up since in a real plasma the number of particles in the Debye cell is large and hence the thermal fluctuation level very low. Either the instability has to be extremely weak or the plasma must already carry a broad band super-thermal noise before the instability sets in. Therefore

in many real experiments not a turbulent but a coherent single mode behaviour with trapping oscillations is to be expected, although the saturation fluctuation level averaged over a trapping period will not be too different from the corresponding quasilinear level, and the averaged distribution function, which is quite insensitive to the form of the spectrum, will show a plateau like form in most cases.

In contrast to the bump-in-tail instability the quasi-linear conditions can never be satisfied for the symmetric two-stream instability since the particles within the range Δv, where diffusion like behaviour is assumed are trapped within a single potential well, $\Delta v \sim \Delta v_{tr}$.

The fact that the first saturation level seen in the numerical simulation of this instability is consistent with the predictions of the quasi-linear equation is not too surprising, since incidentally it coincides with the results of trapping stabilization given by the relation $\omega_b \sim \gamma$. The inapplicability of any weak turbulence theory becomes evident from the strong mode coupling process, which has a coherent not a turbulent character and which persists also for very weak instabilities where a "quasi-linear" phase can hardly be seen. Hence there is some justification for calling certain nonresonant instabilities such as the symmetric two-stream instability "dangerous instabilities".

Acknowledgement

The authors are very grateful to Dr. K.U. von Hagenow for optimizing the numerical code used in the simulation experiments.

References

1 Vedenov, A.A., Velikhov, E.P. and Sagdeev, R.Z.
Nuclear Fusion 1, 82 (1961); Suppl. (1962) 72, 465

2 Drummond, W.E. and Pines, D.
Nuclear Fusion. Suppl. Part 3, 1049 (1962)

3 Dawson, J.M. and Shanny, R.
Phys. Fluids 11, 1506 (1968)

4 Bernstein, I.B., and Engelmann, F.
Phys. Fluids 9, 937 (1966)

5 Morse, R.L., and Nielson, C.W.
Phys. Fluids 12, 2418 (1969)

6 Kadomtsev, B.B., Plasma Turbulence,
Academic Press, London - New York, 1965

7 Shapiro, V.D., and Shevchenko, V.I.
Soviet Phys. JETP, 18, 1109 (1964)

Figure captions

Fig 1 Illustration of the dependence of the nonlinear spectrum on the initial conditions.

Fig 2 Time behaviour of the field energy $W(t)$ of the bump-in-tail instability for a) n_b = 4 %, b) n_b = 5 %, c) n_b = 7.5 % d) n_b = 10 %

Fig 3 Correlation function $g(t,\tau)$ with t = 50 for the case n_b = 5 %, shown in Fig 2b).

Fig 4 Time behaviour of $W(t)$ for n_b = 7.5 %, but with the initial fluctuation level W_o reduced by a factor of 10 as compared with the case shown in Fig 2c).

Fig 5 Trapping oscillations for a single mode case with n_b = 5 %.

Fig 6 The broad spectrum with several peaks of the case shown in Fig 2c , near saturation time (one column for each mode).

Fig 7 $f_o(v)$ for n_b = 4 % a) at t = 0 b) at t = 150; for n_b = 7.5 % c) at t = 0, d) at t = 150

Fig 8 Schematic representation of f_0 and of $E(v) = \int_{-\infty}^{v} dv \frac{v^2}{2} \Delta f_0$ in the resonant region.

Fig 9 Illustration of the development of f_0 in the weak two-stream instability.

Fig 10 Time behaviour of the field energy $W(t)$ (left column) and the square of the potential $V(t)$ (right column) for a) and b) $u = 1.45$, b) and d) $u = 1.5$, e) and f) $u = 1.55$.

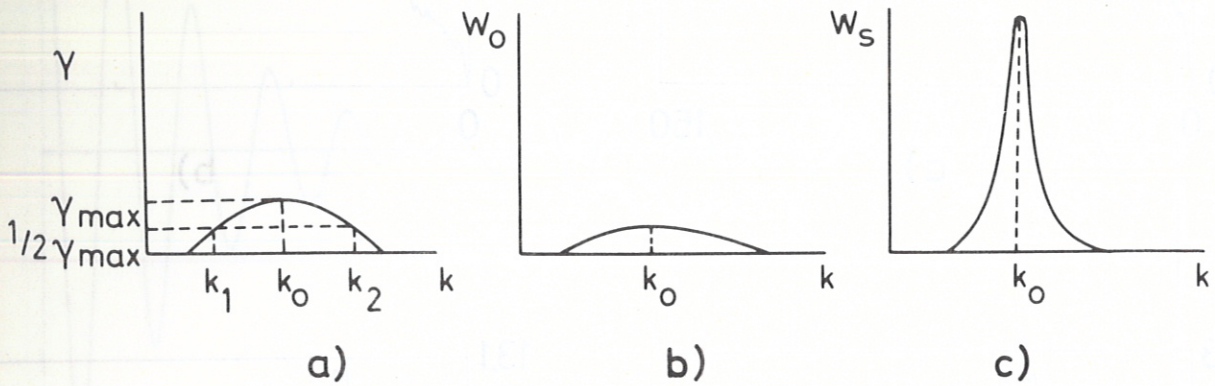

Fig. 1

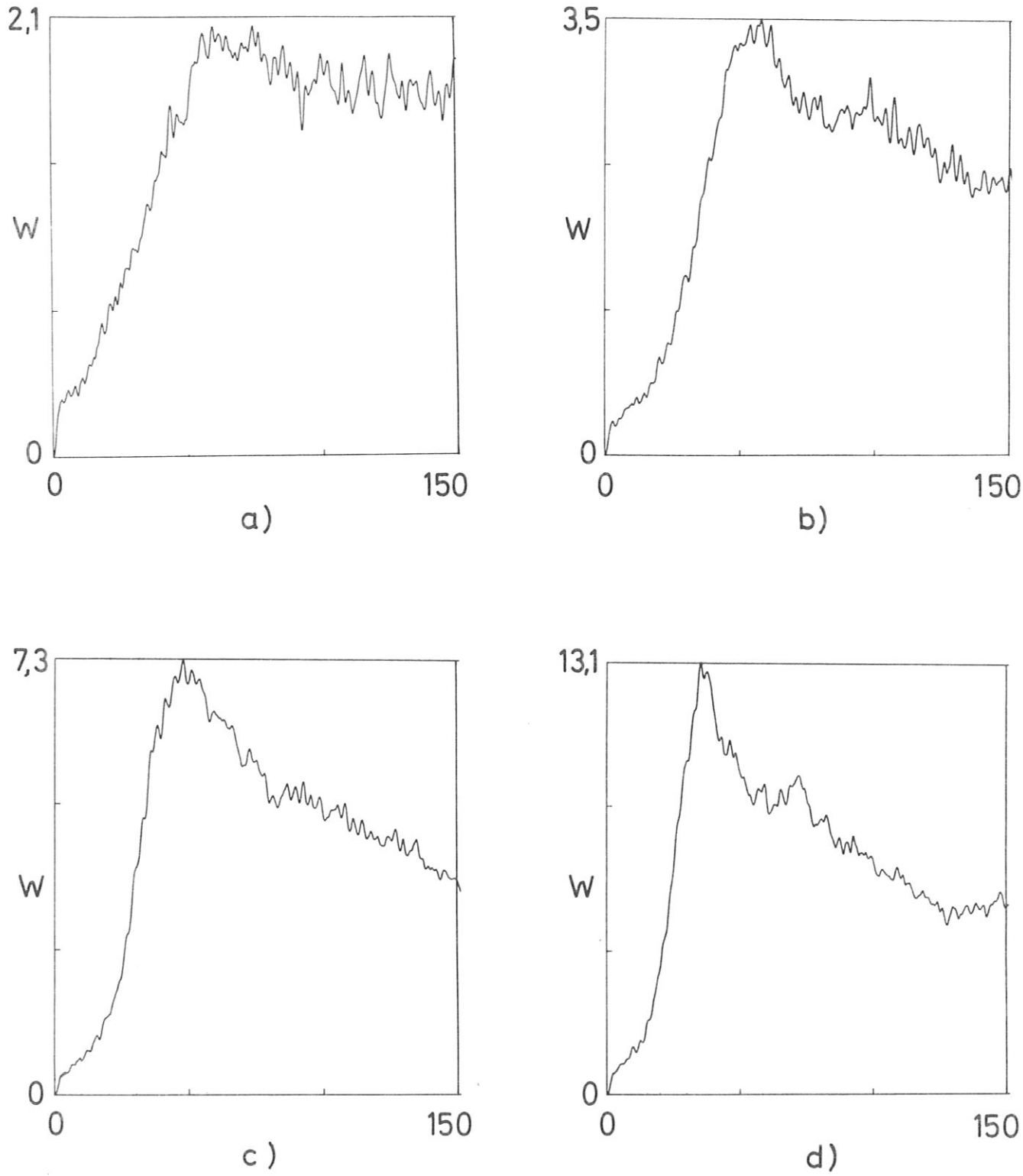

Fig. 2

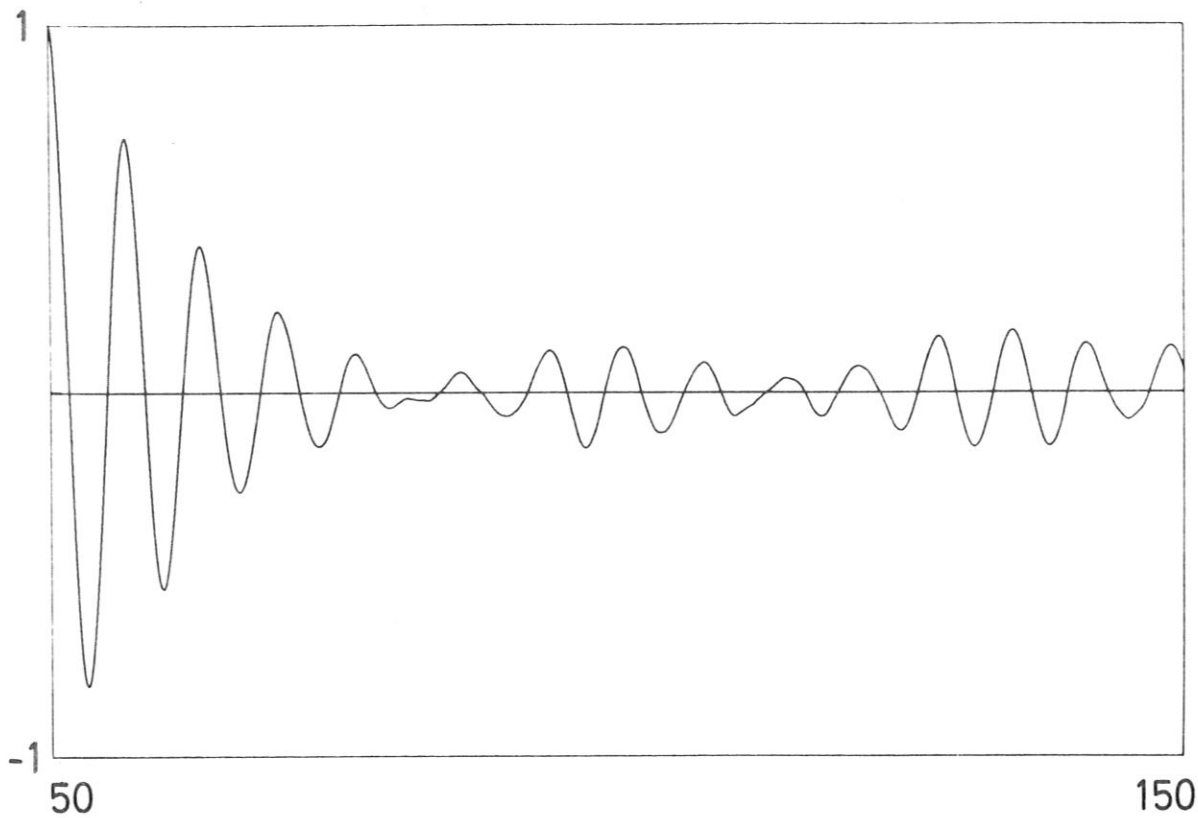

Fig. 3

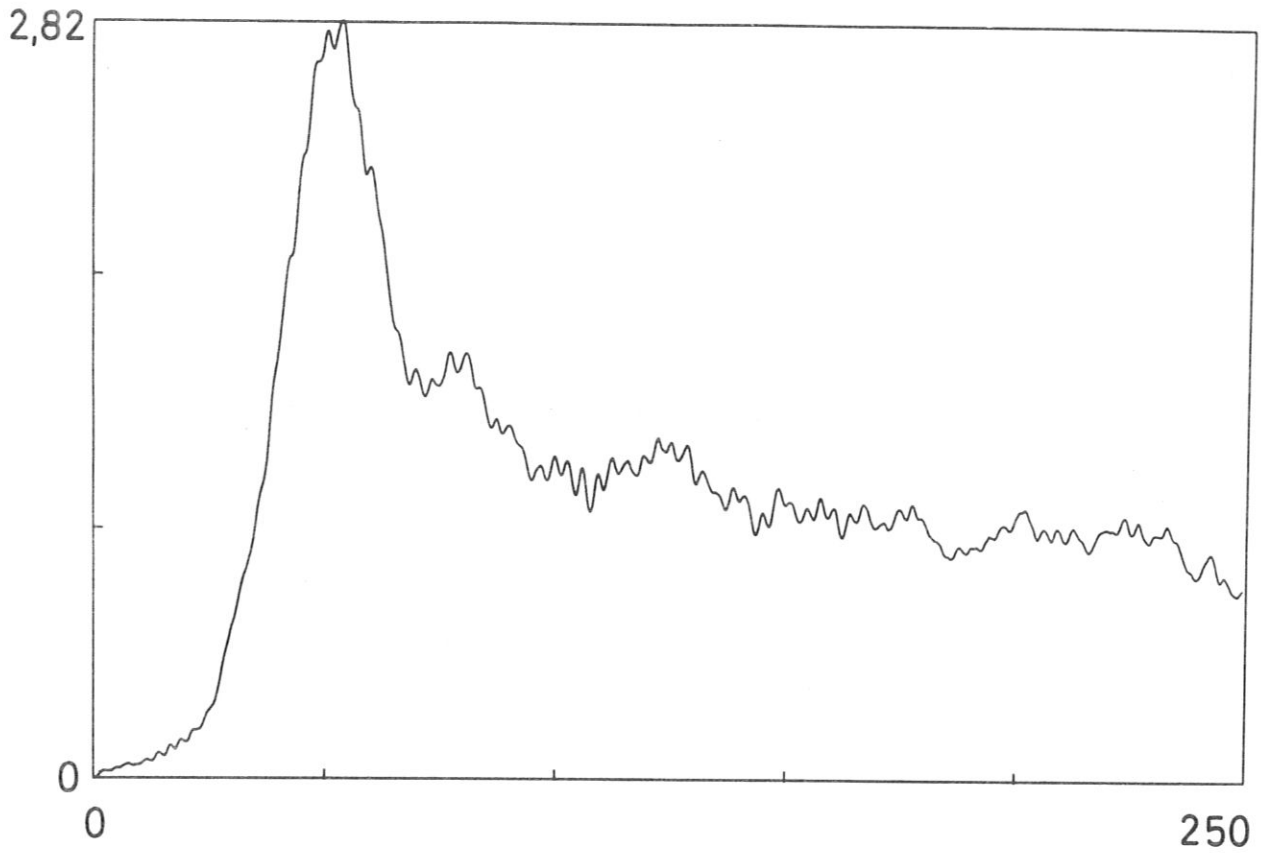

Fig. 4

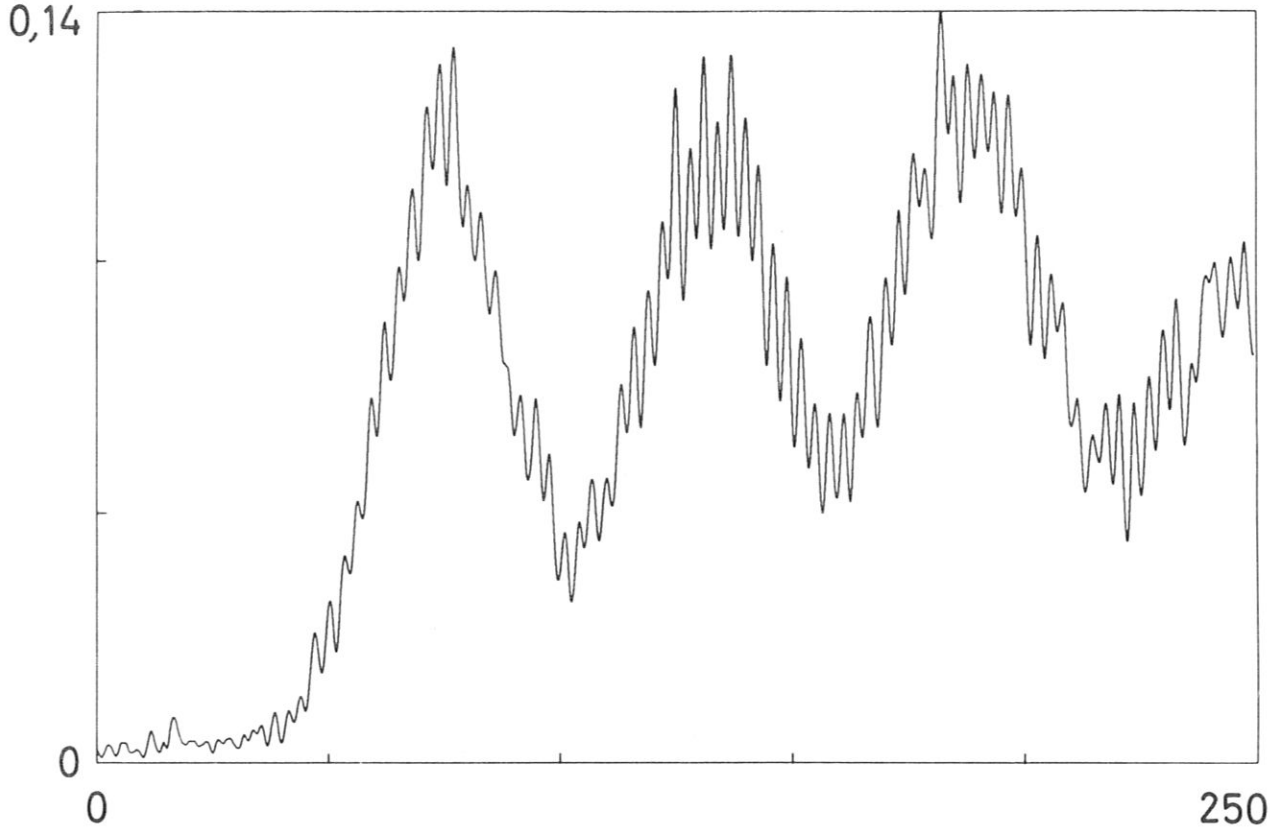

Fig. 5

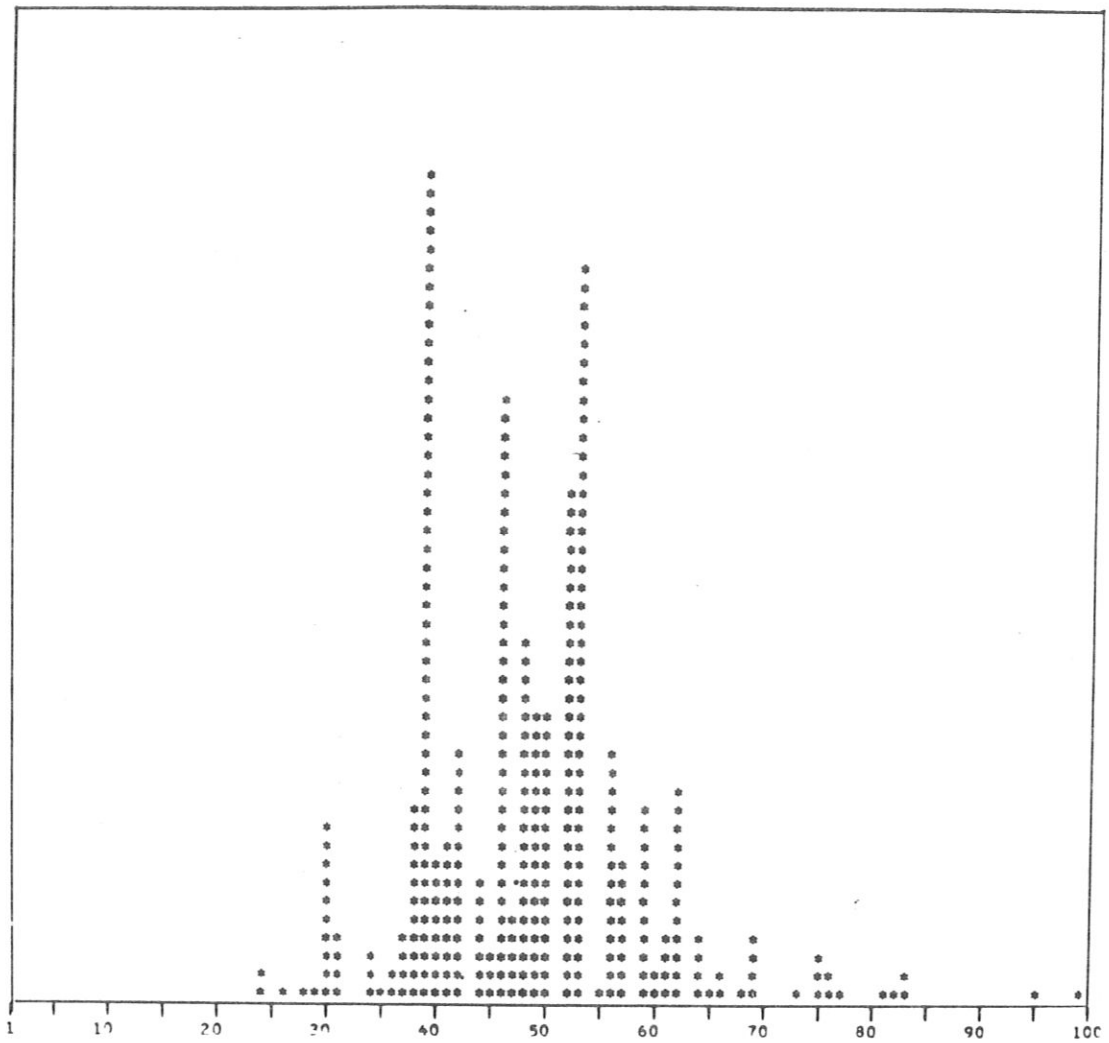

Fig.6

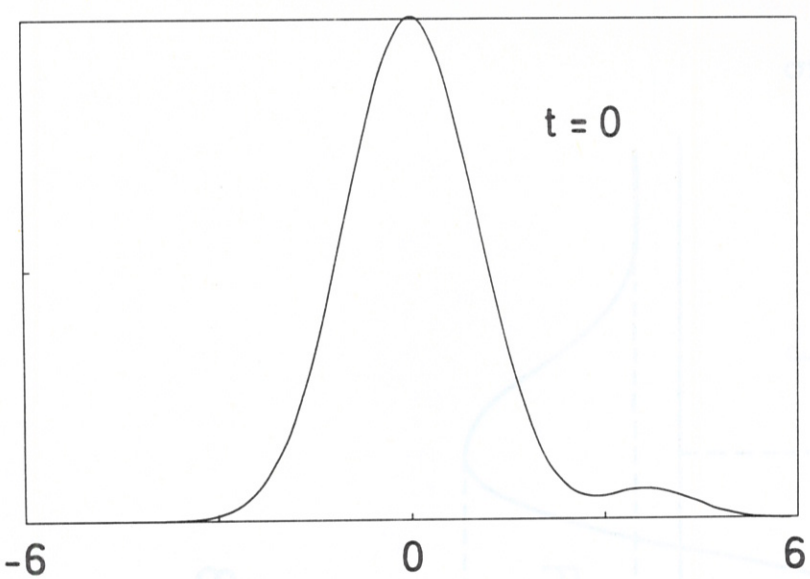

a)

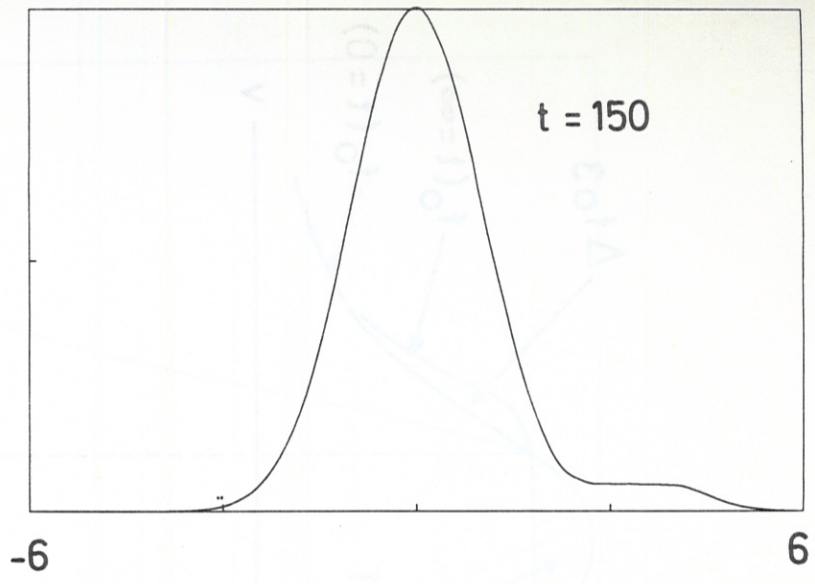

b)

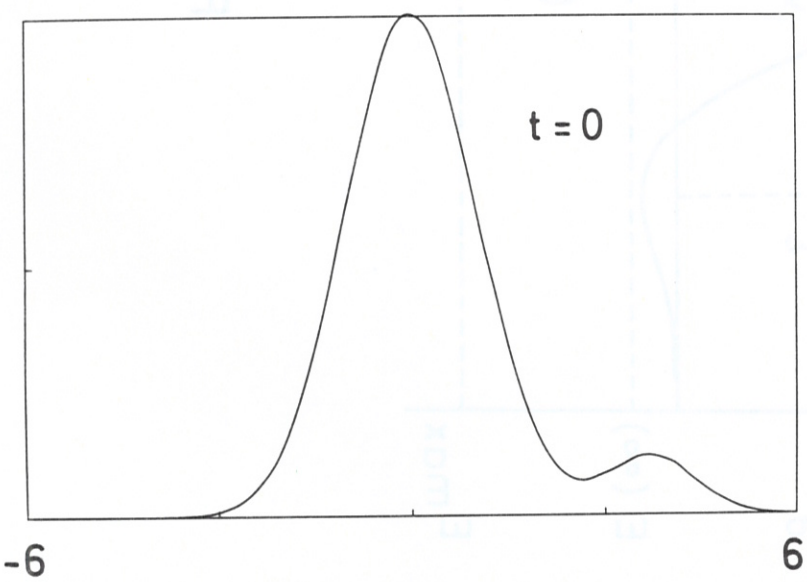

c)

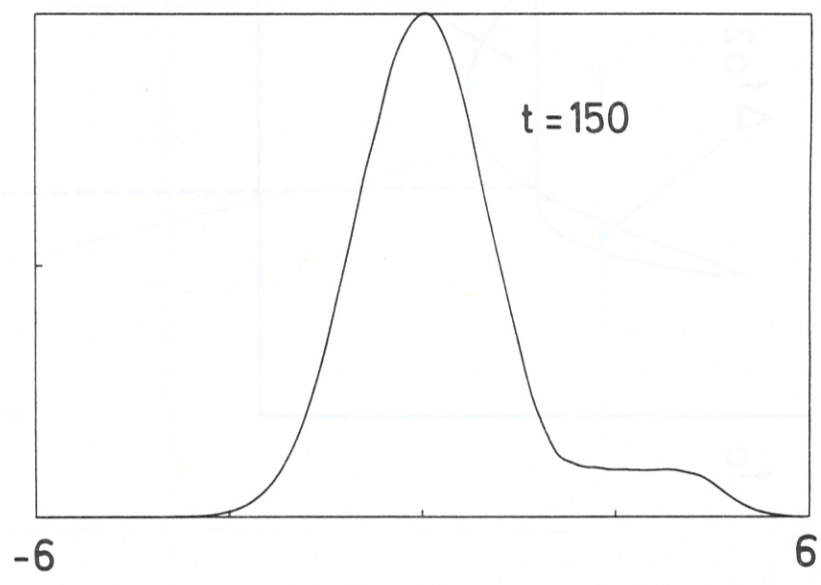

d)

Fig. 7

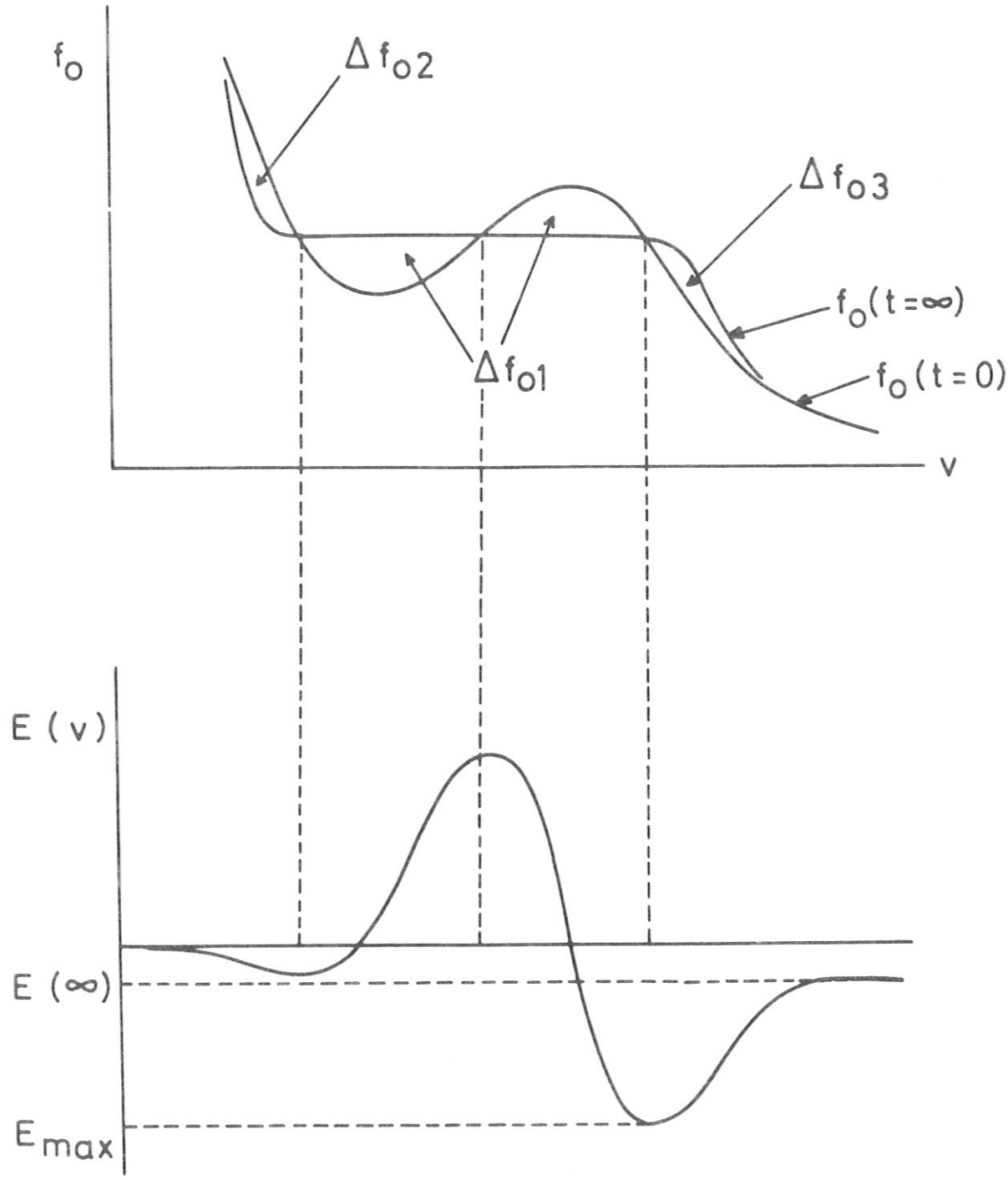

Fig. 8

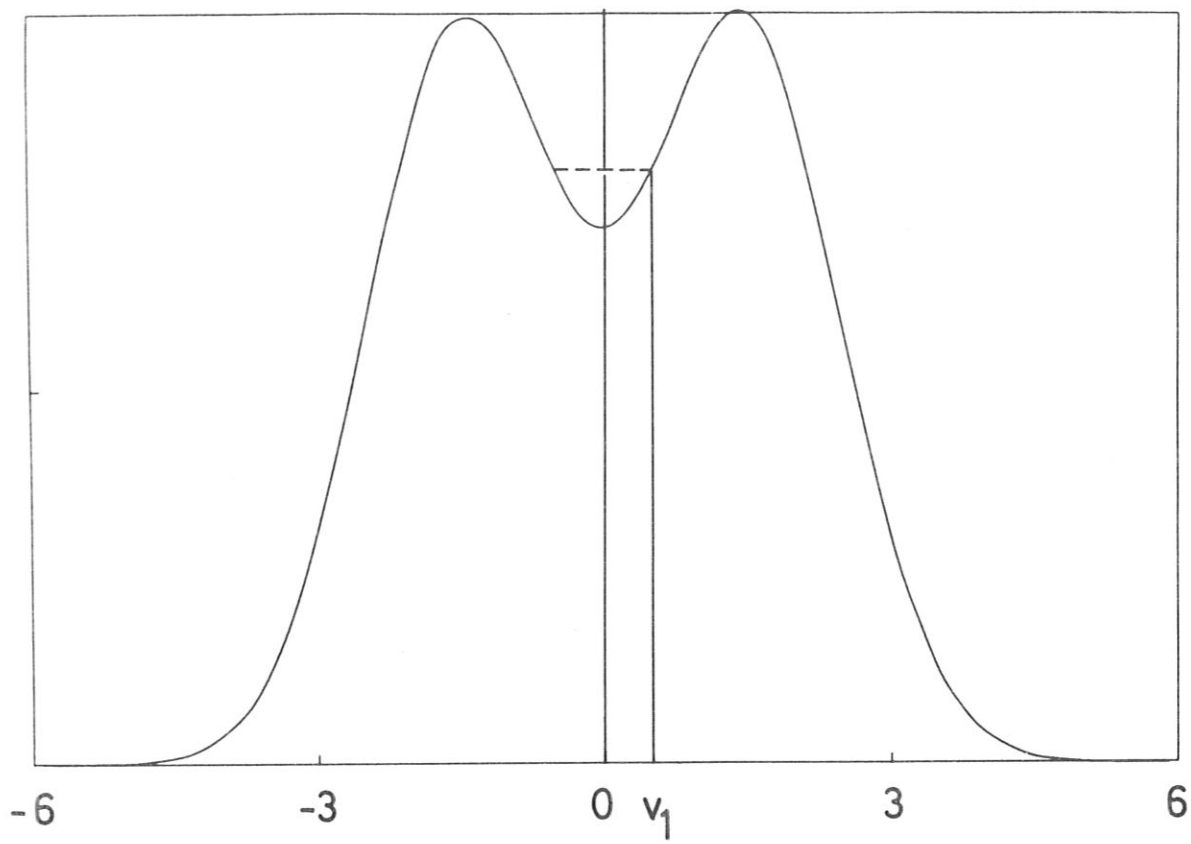

Fig. 9

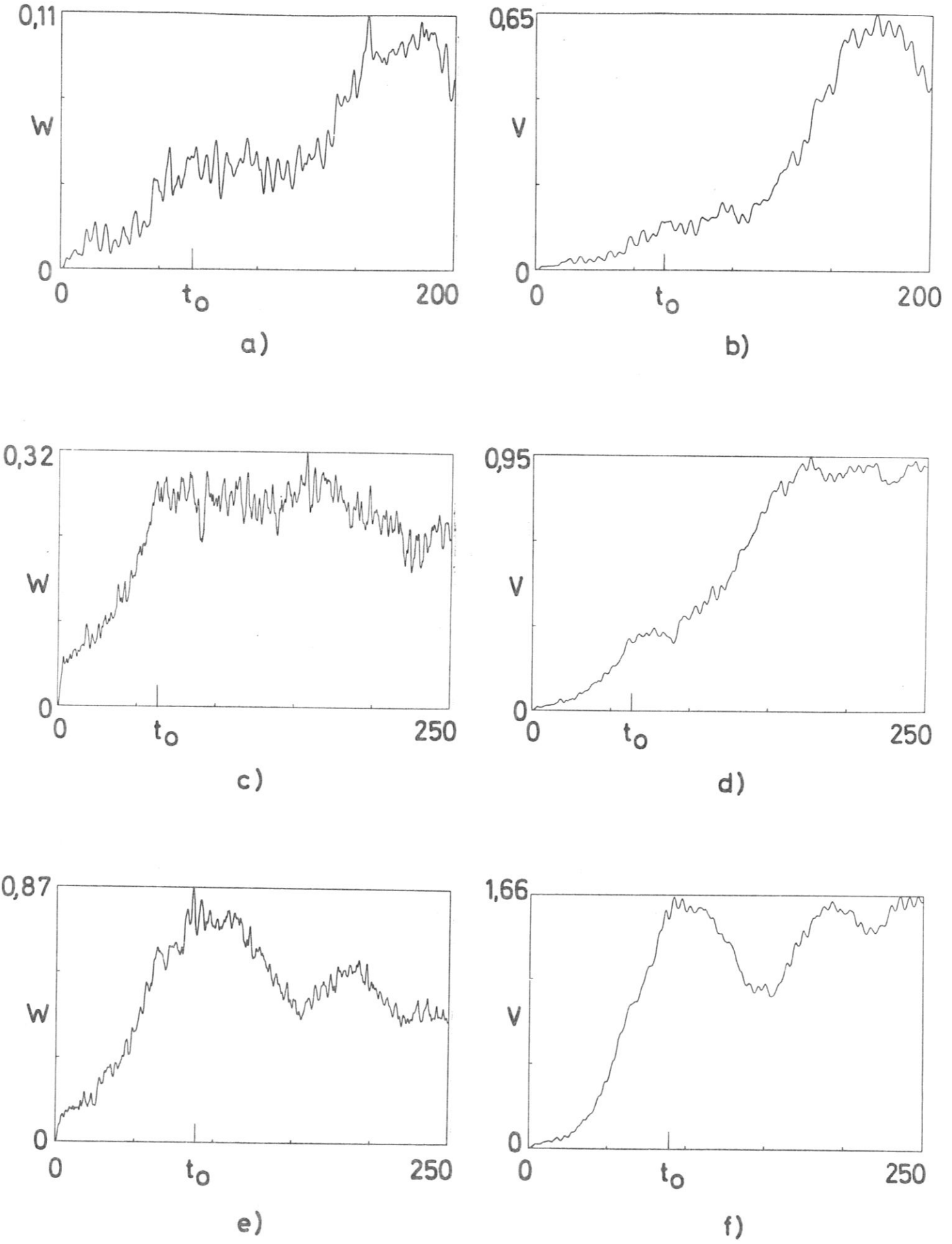
0,11
W
0
0
t_o
200
a)
0,65
V
0
0
t_o
200
b)
0,32
W
0
0
t_o
250
c)
0,95
V
0
0
t_o
250
d)
0,87
W
0
0
t_o
250
e)
1,66
V
0
0
t_o
250
f)

Fig. 10